

A Path to Sustainability: Green Hydrogen Based Production of Steel and Ammonia

Michael Moritz, B.Sc.^a, Jan Raphael Seidenberg, B.Sc.^a, Maximilian Siska, B.Sc.^a, Marc Stumm^a, Song Zhai^a

^aProcess Systems Engineering (AVT.SVT), RWTH Aachen University, 52074 Aachen, Germany

15th February 2020

Abstract: Replacing fossil resources with green hydrogen in industrial production holds tremendous potential for greenhouse gas mitigation. The economic feasibility and greenhouse gas (GHG) mitigation of grid-based electrolytic hydrogen production is highly dependent on the time-variant price and carbon footprint of electricity. In the present contribution, we analyse the economic feasibility of transitioning key carbon-intensive industries, steelmaking, and ammonia production, to green electrolytic hydrogen. Also, we investigate the competitiveness of green electrolytic hydrogen with other environmentally sustainable hydrogen sources derived from biomethane, biogas, and natural gas (associated with carbon capture and storage). We perform process design for steelmaking, ammonia production, and biogas-based steam reforming in order to determine key performance indicators such as costs, conversion factors, and GHG emissions. In particular, we allow for dynamic operation of the industrial processes and hydrogen production to exploit temporal fluctuations in availability, price and carbon footprint of electricity. To this end, we solve bi-objective optimisation problems to determine optimal operational profile and sizing of the industrial processes, hydrogen plants, and (optionally) renewable power generation systems. Case studies are dedicated to the identification of (i) advantages of decentralised renewable energy installations in combination with flexible plant scheduling over steady-state production and (ii) the cost-optimal hydrogen production route. This is done for current (2020) and future (2030, 2050) German energy system scenarios. Based on the analysis results, we outline bottlenecks in sustainable steel and ammonia production and suggest short-term research goals to improve the competitiveness of green electrolytic hydrogen.

1. Introduction

The reduction of anthropogenic greenhouse gas (GHG) emissions is required to counter global warming and climate change. The European Union recently proposed the European Green Deal targeting climate neutrality by the year 2050 to address GHG reduction in policy [1]. Among GHG, carbon dioxide (CO₂) is the main contributor due to its largest position (%) [2]. CO₂ is mainly released during the conversion of fossil resources. The Green Deal targets the decarbonisation of the industrial sector, which holds a share of 9% of the EU's GHG emissions in 2019 [3]. Among various industrial plants, steelmaking and ammonia production heavily rely on fossil resources. Ammonia production utilises carbon-intensive hydrogen from steam reforming of natural gas (NG) while steelmaking consumes coke or natural gas as reducing agents that cause a large amount of CO₂ emissions. Both hold a high potential for cutting emissions as they release 22% and 47% of the European industrial GHG emissions in 2017 [3, 4].

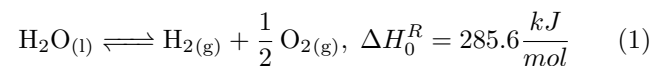
1.1. Literature review

The decarbonisation of steelmaking and ammonia production can be achieved by replacing fossil resources by

renewable hydrogen (H₂). Several ideas utilising renewable hydrogen have been proposed as alternatives to conventional steel and ammonia production in recent years. Also, different routes of low carbon hydrogen production exist.

Decarbonisation of hydrogen production

Nowadays, 95% of the worldwide hydrogen production is based on *grey hydrogen* from steam methane reforming (SMR) or coal gasification. The remainder is hydrogen from sources such as water electrolysis and biomass [5]. Water electrolysis is based on the following redox reaction splitting water into hydrogen and oxygen by the demand for electrical power and heat.

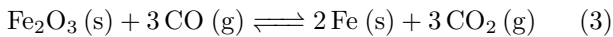
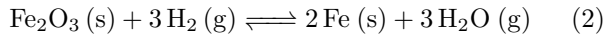


Proton exchange membrane electrolysis (PEMEL) is a mature technology for industrial electrolysis [6]. PEMEL is suitable for flexible operation as they start up in less than 10 minutes [7, 8]. The produced hydrogen is denoted as *green electrolytic hydrogen* if power from renewable energies(RE) is used for electrolysis. Alternatively, *green hydrogen* can be produced from biomass-based gases [9]. Raw biogas is upgraded to biomethane by the removal of impurities and subsequently converted to hydrogen through SMR [10, 11]. Low carbon *blue hydrogen* based on fossil

fuels can be produced by SMR of natural gas with posterior carbon capture and storage (CCS) [12, 13].

Decarbonisation of the steel industry

The decarbonisation of steelmaking demands a retrofit of the existing processes. The steelmaking process consists of two process steps, iron ore reduction and refinement. In the reduction step, iron ore is reduced by the following reactions:



Due to Reaction 3, current steelmaking processes inherently emit CO_2 . Two prevalent steelmaking reduction methods exist, the blast furnace process (BFP) and the direct reduction process (DRP). They use coke and natural gas the reducing agents for BFP and DRP, respectively. The subsequent refinement step is carried out in either a basic oxygen furnace (BOF) or an electric arc furnace (EAF).

Many modifications to both BFP and DRP and alternative processes have been investigated to drastically reduce or even completely avoid GHG emissions. Reports by Yilmaz et al. present the injection of hydrogen into blast furnaces, partially substituting coke as the reducing agent, reducing the GHG emissions by 20% in their simulations [14, 15]. The ULCOS program investigated the recycling of blast furnace off-gas combined with CCS [16]. Partial pyrolysis of coal combined with CCS and biomass as a partial substitute for fossil reducing agents was discussed as part of the HISarna process [16]. Other processes aim at avoiding direct CO_2 emissions altogether by designing new processes. The ULCOWIN process attempts to achieve this by the electrochemical reduction of fine iron ore grains in an alkaline solution [17]. The Plasma Smelting Reduction Process, which Behera et al. [18] recently demonstrated, reduces iron ore in hydrogen plasma, utilising hydrogen more efficiently than DRP. While the processes are promising, they do not pose an option for short term implementation due to their immaturity.

Among the aforementioned alternatives, the most promising and mature technology is the modified DRP which replaces the NG reducing agent with pure hydrogen. This process has been investigated in literature [19–21], and also recognised as a techno-economically promising option by industry representatives [4, 22].

Decarbonisation of ammonia industry

The Haber-Bosch process, known as the most conventional technology for ammonia production, presently covers over 90% of the worldwide ammonia demand and operates

at 150 bar and 450 °C [23] and produces ammonia by reaction 4.



High operating pressure, in combination with an iron catalyst enhances the conversion, while a temperature above 350 °C avoids catalyst poisoning [24].

About 50% of the worldwide production of hydrogen is used in the Haber-Bosch process [23]. While most of today’s ammonia plants obtain their hydrogen from SMR of natural gas [25], other hydrogen sources can be used without sophisticated modification of the existing processes. This means a transition towards other hydrogen sources would have tremendous and prompt impact. Also, introducing green hydrogen has the potential for saving a large amount of GHG emissions because the carbon footprint in ammonia production mostly stems from SMR-based hydrogen production. Therefore, the Haber-Bosch process is considered in this report.

More sustainable production via demand side management

Electrolytic hydrogen is only *green* if the power used for electrolysis has a very low carbon footprint. A high share of renewable energy in electricity production leads to a strong fluctuation in the price and the carbon footprint electricity [26]. The price and carbon footprint of electricity correlates strongly due to the low carbon footprint and the low power generation costs of RE [27]. As outlined by Burre et al. [28], this correlation holds great potential for improvement of the economics and the sustainability of energy-intensive processes by demand side management (DSM).

Brée et al. [29] report that DSM enhances the economics of electrolysis applications by flexible operation. Baumgärtner et al. [30] shows that DSM reduces the CO_2 emissions by exploiting time dependencies in the carbon footprint of the power grid. Additionally, Klauke et al. [31] emphasises the potential of industrial DSM for the integration of renewable energy in the energy system as DSM provides flexible loads. Kopp et al. [6] shows that DSM reduces the hydrogen production costs for water electrolysis considerably. However, large investment costs for electrolysis [8] and high electricity prices compared to natural gas prices [26, 32] are economical inhibitors for green electrolytic hydrogen in many countries such as Germany.

Outline of this report

We investigate the techno-economic and environmental viability of switching steelmaking and ammonia production from fossil to green electrolytic hydrogen. We firstly determine key performance indicators such as costs, energy

demand and GHG emissions for steelmaking, ammonia production and biogas steam reforming by process design. Secondly, we optimise the operational profile and sizing of the industrial processes and hydrogen production. We consider the application of DSM on the production systems. Case studies are envisioned to analyse the trade-off between carbon footprint and production costs of the main products. The potential of electrolytic hydrogen technology is evaluated by comparing it to the optimal system configurations involving not only electrolytic but other also low carbon hydrogen sources for current and future scenarios. Due to its ongoing energy system transition towards renewable energy, we consider Germany as an example to evaluate the European challenges of transitioning from grey to green electrolytic hydrogen.

2. Conceptual process design and simulation

2.1. Process design for steelmaking

The modelled steelmaking process considers the two-step process of DRP and EAF. For the first step, Figure 1 provides an overview of the modelled unit blocks and the material streams between them. First, flowsheet information will be provided for the considered case of a hydrogen feed. Key assumptions will be presented, and the decision to look at synthesis gas as a reducing agent is justified. The corresponding biogas SMR plant is presented afterwards. Then detailed information is given on the chosen reactor model for both considered reducing agents before key assumptions for the EAF modelling are presented.

Direct Reduction Process flowsheet

The main unit operation of the DRP is the shaft furnace reactor. Iron ore is fed to the top of the reactor and partially reduces to iron while travelling down the reactor height. For the proposed use of hydrogen as reducing agent, the reduction is achieved by Reaction 2. Due to the low single-pass conversion of hydrogen, a recycle is applied. Out of the reviewed literature, only Béchara et al. [33] model a recycle stream. Taking a similar approach, we utilise the process flowsheeting software Aspen Plus V.10 [34] for this task, applying the ideal property method.

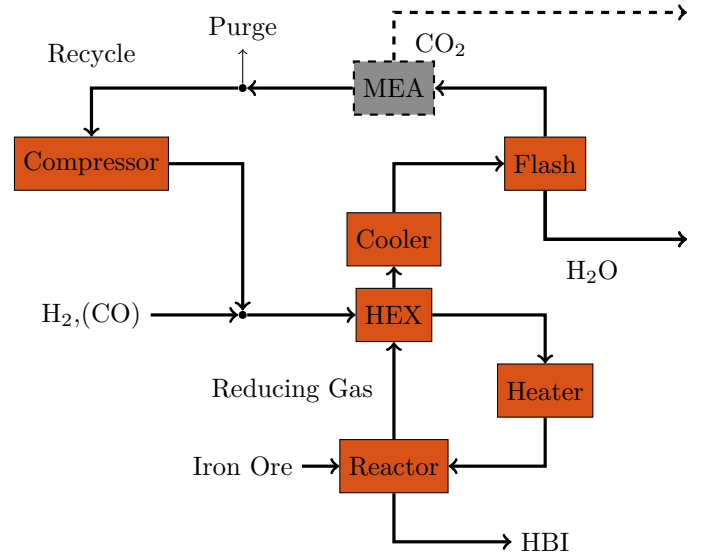


Figure 1: Block flow diagram of the direct reduction process. HEX = heat exchanger, MEA based CO₂ removal unit.

The gas stream leaving the top of the reactor is first cooled to 40 °C before being passed into a flash to separate the water formed by Reaction 2. The reason is that iron reduction is an equilibrium based reaction and higher water content in the reactor feed would lead to less conversion.

The water is then passed to an industrial sewage plant which is not in the scope of this report. The gas phase, consisting of 92% hydrogen and 8% water, is first compressed back to the reactor inlet pressure in a single-stage compressor before being mixed with the hydrogen feed. The resulting reducing gas stream is then heated to the reaction temperature by the heat of natural gas combustion and fed to the shaft furnace. Literature selects inlet gas temperatures from 1070 K [21] up to 1,230 K [35]. As part of this report, the reducing gas inlet temperature is raised to 1,300 K to prevent water condensation in the reactor gas outlet due to the endothermic nature of the hydrogen-based reduction reaction.

Process design for hydrogen based on steam reforming

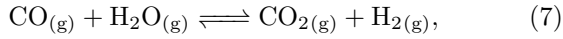
As a feature of this report, biogas based synthesis gas is also considered as a reducing agent. In terms of the flow-sheet, very little changes as only a carbon capture unit in the form of a monoethanolamine (MEA) based acid gas scrubber is needed for CO₂ removal, again necessitated by reaction kinetics. The synthesis gas feed is taken from a biogas SMR, whose model is described in detail the following section.

We include process models for steam reforming to this report since we consider hydrogen, natural gas, biomethane and biogas. Steam reforming of methane to hydrogen relies

on the Sabatier reactions [36]:



$$\Delta H_{\text{R}}^\circ = -206.1 \frac{\text{kJ}}{\text{mol}} \quad (6)$$



$$\Delta H_{\text{R}}^\circ = +41.15 \frac{\text{kJ}}{\text{mol}} \quad (8)$$

(9)

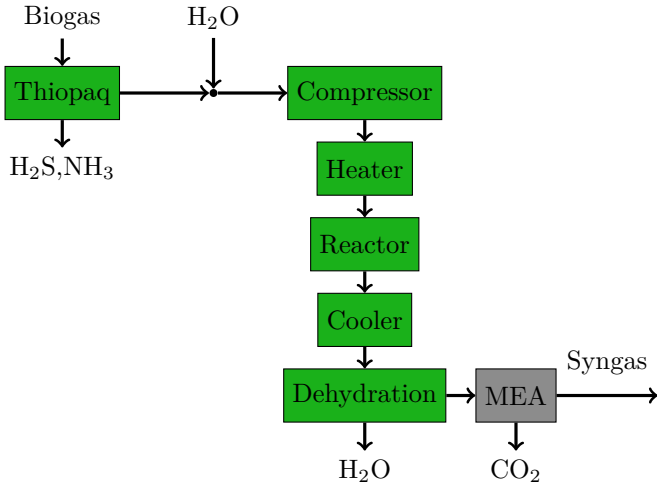


Figure 2: Block flow diagram of the biogas steam reformer with integrated biogas upgrading. MEA = MEA CO₂ based capture unit.

Methane and water are converted to CO₂ and hydrogen. We refer to existing work by Roh et al. [37] to model a conventional SMR process. The SMR can utilise natural and biomethane as educts to generate hydrogen or synthesis gas. Raw biogas consists mainly out of CH₄ and CO₂ but also contains a considerable amount of impurities such as H₂O, NH₃, O₂, H₂ and H₂S [38]. Biomethane is produced by biogas upgrading by the removal of H₂S, NH₃ and CO₂. Not only hydrogen but also carbon monoxide (CO) is an educt for synthesis gas based steelmaking. Steam reforming to synthesis gas can be enhanced by converting the CO₂ content of raw biogas directly to CO before removing it. We design a biogas reformer which integrates biogas to SMR to exploit the full chemical conversion potential. The Thiopaq [11, 39] technology is used for biological removal of H₂S and NH₃. Subsequently, the biogas is converted to a hydrogen, CO and CO₂ rich stream in a single reactor. After that, the stream is dehydrated. At last, CO₂ is removed by a MEA based CO₂ removal (or capture) unit. We model the biogas reforming process in Aspen Plus V.10 using the Peng-Robinson equation of state for thermodynamics. The reactor is modelled by the RGibbs reactor model. We utilise split factors from literature to model the MEA unit [40]. The desulphurisation reaction within the Thiopaq

process is modelled by the RStoic reactor model [11, 39]. Gas dehydration is modelled by a flash unit with subsequent triethylene glycol absorption for dehydration which is modelled by split factors from literature [41]. Energy integration is performed using the Aspen Energy Analyzer. We obtain synthesis gas consisting to 81 mole-% of hydrogen and 18 mole-% of CO.

Shaft furnace model

The unreacted shrinking core model is the most prevalent reduction model for gaseous reduction agent-based iron reduction [35, 42–45]. It models the shaft furnace as a fluidised bed reactor, simplifying reaction steps and transport effects by applying the following assumptions [35, 42]:

- Mass and heat transfer resistances through the film around the solid particle are negligible compared to diffusional resistance inside the porous solid.
- Only steady-state operating conditions will be considered.
- Plug flow is assumed for gas and solid phase.

As the resulting fluidised bed reactor still uses heat and mass transfer equations, the reactor models embedded in Aspen can't be used. Instead, we implemented a (customized) reactor model in Matlab. While the discussion about the benefits of hydrogen-based iron reduction can be frequently found in literature [19, 46], few papers [20, 21] have modelled this process so far. To the best of our knowledge, we are the first to model a full DRP, including a rigorous shaft furnace model. Since the unreacted shrinking core model is utilised to model the reduction process by synthesis gas, as a feature of this report, the model is modified to be applicable to the reduction by pure hydrogen. Given the innovation of the pure hydrogen-based reduction process, there is a lack of consistent parameters. It is a common approach to model the shaft furnace based on MIDREX plant data [19, 21]. As such, we utilise parameters for the Siderca steel plant reported by Parisi et al. [35]. Similarly, yearly production of 800 kt of liquid steel is assumed.

The resulting model is one dimensional discretized over the height of the reactor. Differential equations describe the spatial variation of the concentrations of educts and products as well as solid and gaseous phase temperatures. Detailed equations can be found in the Supporting Information.

The resulting system of ordinary differential equations is solved in MATLAB [47] as a boundary value problem with the corresponding bvp5c solver. Results for a synthesis gas feed compare favourably with the results of Parisi et al. [35]. Reactor results are passed to MATLAB with the MATLAB/Aspen Plus V.10 interface. The flowsheet was

converged iteratively using the same interface. See supplementary information for the converged flowsheets.

2.1.1. Electric arc furnace model

In the second step of the process, reduced iron which is leaving the shaft furnace is compressed to the so-called hot briquetted iron (HBI), instead of iron sponge due to superior storage properties. The HBI is fed to the batch-wise operating electric arc furnace (EAF). The EAF has been modelled with different levels of detail. To better reflect the costs associated with green electrolytic hydrogen, this report assumes that no scrap can be utilised for the smelting operation and modifies the model provided by Vogl [21] to this end. This results in the highest possible electricity demand, but also in a clear cost associated with the replacement of synthesis gas with green electrolytic hydrogen.

2.2. Process design for ammonia production

Process simulations are conducted in Aspen Plus [34] using the Redlich-Kwong-Soave equation of state with Boston-Mathias modification, because the ammonia process is a gas reaction, its species are slightly polar and the process is operated at high pressure. Yearly production of 475 kt is assumed, which is a typical production capacity in industry. Figure 3 shows the block flow diagram of the designed process. The educts are compressed to assumed 250 bar and mixed with a recycle stream. After that, they are fed to the reactor sequence operating at 350 °C. The enriched product stream is separated by flashing the product at assumed 0 °C. Afterwards, a small fraction of the vapor recycle stream is purged. The remaining stream is compressed and heated to operating conditions. The product-enriched liquid bottom stream is flashed a second time at a lower pressure so that the outgoing bottom stream meets the product specifications of 99.98% purity [48]. The waste gas streams containing hydrogen, nitrogen and ammonia are assumed to be burned since they do not contain any carbon. The waste treatment step is not included in the analysis.

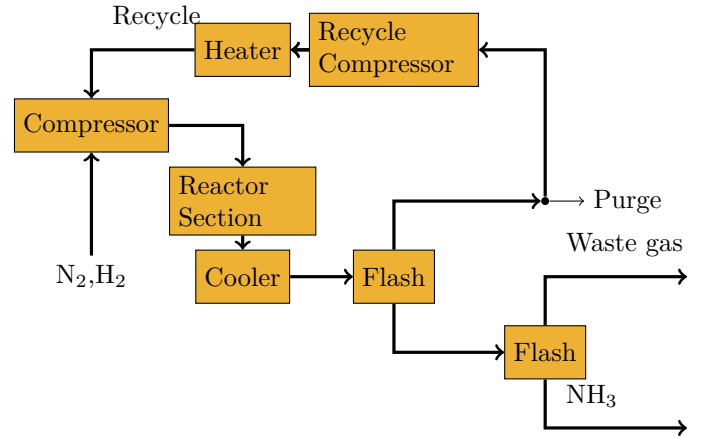


Figure 3: Block flow diagram of the ammonia process.

Ammonia reactor

A plug-flow reactor (RPlug) is used to model the reactor. We use a reaction kinetic model to determine the reactor size rigorously. The following reaction kinetic proposed by Nielsen [24] is chosen:

$$r = A_c \left[\frac{AK(a_N k_{eq}^2 - \frac{a_A^2}{a_H^2})}{(1 + K_a \frac{a_A}{a_H})^{2\alpha}} \right] \quad (10)$$

Where A_c is the catalyst activity and is chosen as 1. ω is taken as 1.523 and α as 0.654. a_N , a_H and a_A are functions of the mole composition, pressure and temperature. The specific rate constant AK , the adsorption equilibrium constant K_a and the equilibrium constant k_{eq} are functions of temperature. The equation is valid for temperatures above 350 °C. A reactor temperature below that value should not be reached in any case, because the catalyst will be poisoned and thus reaction is slowed [24].

The reaction kinetic is used to plot isobaric single-pass conversions against temperature. Thereby, we see a high single-pass conversion at a reaction temperature of 350 °C and set this as the reactor temperature. A similar procedure is conducted to plot adiabatic single-pass conversions against residence times to choose an appropriate residence time and thus the reactor size.

Since an adiabatic plug flow reactor is used and the Reaction 4 is exothermic, the reactor has to be split into multiple plug flow reactors with coolers in between. We choose three reactors.

3. Production cost and carbon footprint calculation

3.1. Production cost

We estimated the investment costs for the steel and ammonia process according to Guthrie’s method [49]. The

steel reactor is solely accounted for by a different method (see 3.1). Cost calculations are performed in 2018 Euros. Guthrie’s method is used for installation costs of reactors, flash vessels, heat exchangers and compressors. Peripheral cost are accounted for by the Lang factor of 4.74 for ammonia and 3.63 for steelmaking [50]. Operating costs can be divided into utility costs, maintenance costs and labour costs. Utility costs for heating and cooling are taken from Aspen Plus while the electricity costs are calculated with the marginal cost of 0.04 €/kWh, the mean marginal cost in Germany 2018 [32]. The maintenance costs are taken as 3% of the capital costs [51]. The labour costs are calculated as outlined in [49] and a labour cost factor of 43.52 \$/h is taken [50]. A detailed table of cost parameter and sources are given in the Supporting Information.

HBI of the steelmaking process can be stored easily, so its storage costs are assumed to be negligible. NH₃ can be stored in liquid form at ambient temperature and around 9 bar [52]. The NH₃ leaving the Haber-Bosch process is already in that condition, so cost-wise only the tank has to be considered. The tank cost is taken as 0.1423 €/kgNH₃ based on data of Morgan et al. [53].

Guthrie’s cost estimation method generally results in concave functions with respect to capacities. Linear over-estimation is achieved by (i) calculating the linear regression and (ii) shifting the regression line upwards so that costs are overestimated by regression line. The resulting parameters are presented in the Supporting Information.

Costs for steel reactor

The investment costs for the DRP including the recycle and the EAF are calculated with data from Vogl et al. [21]. Operational expenditures (OPEX) are determined by the following procedure: (i) calculating the operating point by the unreacted shrinking core model (ii) calculating the stoichiometric factor similar to Vogl et al. [21] (iii) calculating the needed gas stream to react one ton of iron ore per hour (iv) transferring calculated gas stream to Aspen Plus (v) recording OPEX associated with the recycle. This procedure is repeated for different production rates.

3.2. Carbon footprint calculation

The carbon footprint of our products is calculated by accounting for the carbon footprint of incoming streams into the system and of operating plants.

We assume that the plants emissions are solely accounted for operation and not for plant installation and deconstruction. While operating a plant, its emissions can be distinguished by inherent and avoidable emissions. The latter depends on the choice of its feedstock, whereas inherent emissions cannot be changed.

Their cradle-to-gate carbon footprint accounts for incoming streams. Electricity from the power grid, biomass and

natural gas are accounted for because they influence the carbon footprint of the respective hydrogen and thus the decision which plant to build. Nitrogen and iron ore are excluded because they cannot be substituted in the regarded processes.

4. Optimal scheduling and sizing

4.1. Assumptions

We assume for the DSM model that the electricity cost, carbon emission, availability of renewable energy sources are exogenously given and perfectly forecasted. Additionally, we assume that nitrogen is bought from a cryogenic air separation plant which is not part of the optimisation model. Finally, we took our costs for the ammonia and steelmaking plant from our cost model (see Section 3.1) and the CCS and SMR/BM-plant from surrogate cost-models from Hasan et al. [54] and Murthy Konda et al. [55].

4.2. Surrogate modelling

Dynamic steelmaking

Flexible plant operation in the context of DSM can drastically reduce electricity costs [28]. However, no literature could be found on flexible load management for direct reduction processes. Millner et al. [56] recently published new technology currently being implemented in MIDREX plants. Among the proposed technologies are both a new control system and a model for predicting metallisation and carbonisation of the HBI. Given these recent advances, we assume that slight changes in the production rate are possible. A maximum hourly load change of 1% is allowed in this report. The level of load change is critical to metallisation and flexibility. Our preliminary tests varying solid throughput of the shaft furnace model by +/- 20% resulted in a maximum deviation of 4% less metallisation. As such, the energy needed by the EAF is calculated to be correspondingly higher. To include higher load change rates, a dynamic process model including a control structure must be investigated. Such a model is outside the scope of this work.

Dynamic ammonia production

In the context of modelling DSM, the load change rate and load bounds of the ammonia plant has to be considered. Industrial Haber-Bosch plants already operate on a load range of 65-100% [57]. Based on Schulte Beerbühl et al. [58] a load range of 20-100% is considered. Another factor constraining the dynamic production is given by the process response to step-changes in the production rate. Luyben [59] reports a settling time of approximately three hours after a step-change in the production rate of 15%.

Subsequently, a maximum load change rate of 5% per hour is assumed.

4.3. Optimisation problem formulation

Model description

We consider a time interval of 8,760 hours, which corresponds to one year. The steel has to generate a fixed amount of product during this year while the ammonia plant must provide a constant product stream. Ammonia and steel optimisation models are implemented separately. Figure 4 shows a combined block flow diagram and the system boundary considered in this work.

In both models, the plants can choose between hydrogen from electrolysis or hydrogen from SMR. The electrolysis has a variable production rate $PR_{EL(t)}$ and size S_{El} . It covers its power duty by the power grid, its own offshore, on-shore wind park or photovoltaic (PV) plant. Water costs of electrolysis are considered. The size of RE plants $S_{(RE)}$ is a variable and their electricity production $PR_{(t,RE)}$ depends on the availability $a_{(t,RE)}$ of wind and solar. Produced hydrogen is buffered in the hydrogen storage variable in size S_{SH_2} .

In the steel model, the process can be operated by using synthesis gas or a mixture similar to synthesis gas containing a higher mole fraction of hydrogen. Synthesis gas is either attained from the reforming of BG or NG. A higher mole fraction of hydrogen is possible by utilising electrolysis. The steam biogas reformer (SBR) is variable in size S_{SBR} and production rate $PR_{SBR(t)}$. Synthesis gas is assumed to be storable in the hydrogen storage.

The DRP consumes hydrogen and fuel for heating to reduce iron ore and thereby emitting GHG. The intermediate product HBI which is buffered and then fed to the EAF which is variable in size S_{EAF} . The production rate $PR_{EAF(t)}$ defines the withdrawal from the HBI storage and the power duty of the EAF. The product of the EAF is liquid steel measured by the stream $\dot{m}_{LS(t)}$. The batchwise operation of the EAF is ordinarily modelled with integer variables. This significantly increases the computational burden as it shifts the model from LP to MILP. Instead, we assume the plant runs two EAFs. When one EAF runs, the other one is prepared for operation and vice-versa. In the ammonia model, the SMR with size S_{SMR} can either utilise biomethane (BM) or NG. CCS can be used to reduce the CO₂ emissions of the SMR plant. The amount of BM and NG fed to the SMR is defined by $PR_{amm(t)}$ and $PR_{NG(t)}$. The ammonia plant consumes nitrogen from cryogenic air separation, electric power and fuel for heating to produce ammonia. Subsequently, the product is buffered in an ammonia storage which is drained by the constant product flow \dot{m}_{NH_3} . Carbon emissions from the SMR, DRP, EAF and the ammonia plant are included in emission trading with the CO₂ price P_{ET} . The carbon storage price P_{CS}

applies on captured CO₂ from the carbon capture unit of the SMR.

Decision variables

Decision variables are grouped into a time-dependent vector $\mathbf{x}(t)$ and a non time-independent vector \mathbf{y} . The latter contains the sizes of the plants and equipment units i represented by the variable S_i . $\mathbf{x}(t)$ contains production rates of the plants and equipment units i which are denoted by $PR_{(t),i}$. For the ammonia model a binary variable exists determining the installation of SMR y_{SMR} . The Supporting Information summarises all optimisation variables and their bounds.

Formulation of bi-objective problem

We modelled the problem in GAMS 28.2 and used the solver CPLEX 12 [60]. The optimisation models are formulated in the product space as suggested by Mitra et al. [61]. By this, we shift the computational expenses of solving energy and mass balances from the optimisation models to the plant models. We obtain surrogate functions to describe the feasible region in the optimisation models. Thus, we can formulate the steel optimisation model by linear programming (LP) and the ammonia optimisation model by mixed integer linear programming (MILP) with just a single binary variable (y) as the decision variable for building a SMR. We perform bi-objective optimisation to evaluate the trade-off between production costs and the product's carbon footprint. The first objective is the production cost measured in €/tonne liquid steel or ammonia produced. Carbon footprint is the second objective and is measured in tonne CO₂ equivalent per tonne liquid steel or ammonia produced. It is discretised as an epsilon-constraint. For the sake of simplicity, we present the steel model briefly. The optimisation is formulated as followed.

$$\begin{aligned} \min_{\mathbf{x}(t), \mathbf{y}} \quad & \left\{ \begin{array}{l} \text{Production cost} \\ \text{Carbon footprint} \end{array} \right\} \\ \text{s. t.} \quad & \text{Operation constraint} \\ & \text{Mass balances} \\ & \text{Energy balances} \end{aligned} \quad (11)$$

The production cost is calculated by the following equation

$$PC = \sum_t \frac{CAPEX + OPEX(t) + EPEX(t)}{m_p(t)} \quad (12)$$

with production cost (PC) in 2018€, capital expenditures (CAPEX) in 2018€, OPEX in 2018€, electricity expenditures (EPEX) in 2018€, and mass flow of product $m_p(t)$ in tonnes of product. The operation constraint contains the

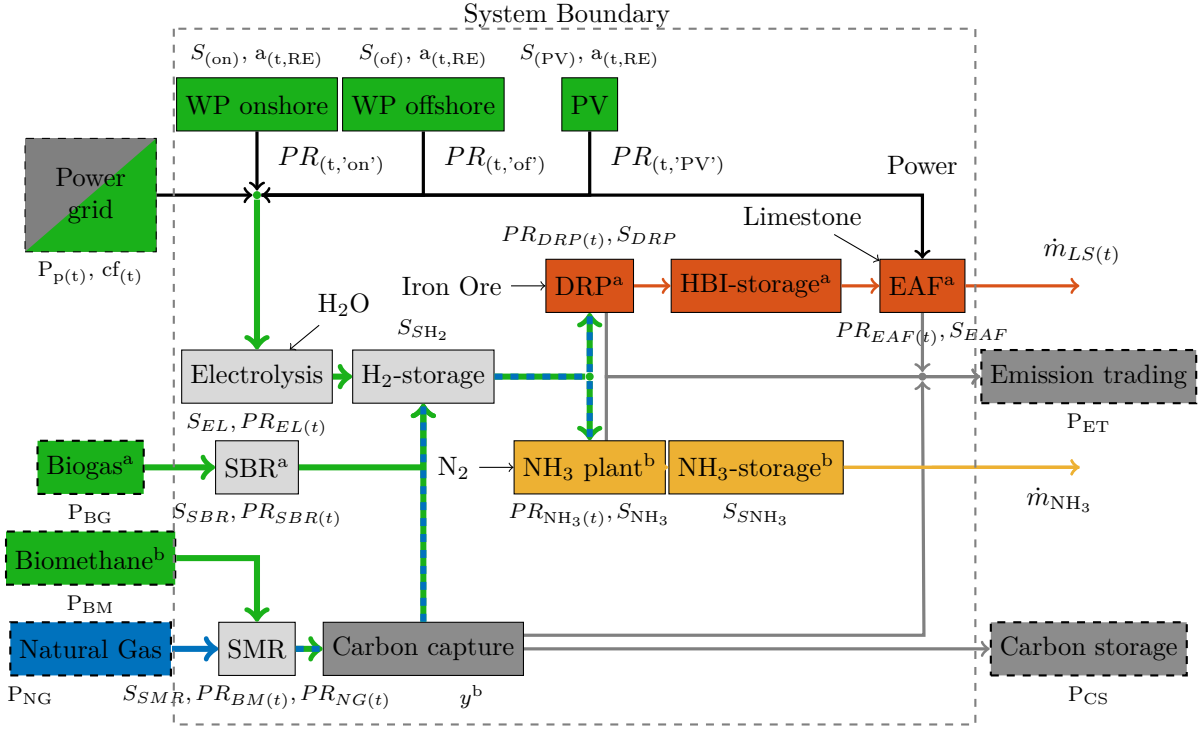


Figure 4: Combined flowsheet of the steel and ammonia optimisation model. Arrow colours refer to electricity (**black**), green hydrogen route (**green**), blue hydrogen route (**blue**), ammonia route (**orange**), steel route (**red**) and CO₂ route (**gray**). Dashed boxes outside the system boundary are data sources. Variables are written in italic letters. ^a:only present in steel model. ^b:only present in ammonia model.

technically allowed loads and rates of load change of each unit in our system. Additionally, the produced electricity of RE is constrained by the availability $a_{(t,RE)}$ and production rates of units are limited by their capacities.

5. Case study

To evaluate the change to environmentally sustainable hydrogen-based production of steel and ammonia, we define the base case (BC-EL) as steady-state operation utilising green electrolytic hydrogen from grid power only, electrolysis with DSM (DSM-EL) and optimised systems containing all technologies depicted in fig 4 (DSM-OS). By comparing them the economic viability of green electrolytic hydrogen is analysed against alternative CO₂ mitigating hydrogen sources.

Table 1: Overview of included technologies for each system. ET = emission trading, P = power grid, DSM = demand side management, RE = renewable energy, BG = biogas, BM = biomethane, NG = natural gas and CCS = carbon capture and storage. For Steel DSM-OS* natural gas and biogas is converted to synthesis gas.

Steel	ET	P	DSM	RE	BG	BM	NG	CCS
BC	X	X						
DSM-EL	X	X	X	X				
DSM-OS*	X	X	X	X	X		X	X
Ammonia	ET	P	DSM	RE	BG	BM	NG	CCS
BC	X	X						
DSM-EL	X	X	X	X				
DSM-OS	X	X	X	X		X	X	X

Given the recent emergence of large scale PEM electrolysis, investment costs are expected to reduce over the next decades [5, 8]. Tsiropoulos et al. expect the costs associated with installing renewable energy capacities to slightly reduce [62]. The energy transition in Germany constantly reduces the carbon footprint of electricity and is influencing the prices. Due to the dates proposed in the Green Deal [1] future scenarios until 2050 are considered., we evaluated the scenarios 2020, 2030 and 2050. The hourly marginal

costs and carbon footprint of electricity is provided by Böing et al. [32]. Future prices for natural gas and emission trading are taken from Schlesinger et al. [63]. Prices for biomethane and biogas are taken from the Agency for Renewable Resources [64] and Adler et al. [38]. Carbon capture and compression costs are calculated according to Hasan et al. [54]. The costs for carbon storage are estimated corresponding to Bui et al. [65].

5.1. Steelmaking

BC vs DSM-EL

In this section, we analyse the potential benefits of DSM on the economic and environmental viability of electrolytic hydrogen production. For this reason, we compare the base case with the system EL.

The top half of Figure 5 shows the optimisation results of all considered systems for the three scenarios 2020, 2030 and 2050 as pareto fronts. A pareto front is defined as the set of points from which none of the investigated criteria can be improved without worsening at least one of the others. As a first case study, we compare the base case, represented by a black cross, against the DSM-EL system, which is represented by red lines. It can be seen that the production costs of the base case rise and its carbon footprint declines from scenarios 2020 to 2050. For the DSM-EL system, we observe that production costs increase with decreasing carbon footprint for all scenarios. This trend is due to grid power gradually being replaced by renewable energies reducing the carbon footprint but increasing the costs (cf. Supporting Information). In scenario 2020 minimal production costs are achieved utilising grid power only, as it is cheaper than installing renewable energy capacities. At minimal carbon footprint, the energy demand is completely satisfied by the installed renewable energies, leading to the highest production costs. The reader is referred to as the energy supply steal plant plot for the DSM-EL system in the year 2020 in the Supporting Information.

For 2030, the lowest possible production costs increase alongside a decrease in carbon emissions compared to 2020. This is because rising mean power prices are accompanied by the power grid’s decreasing carbon footprint. Installing renewable energies dedicated to the steel plant is economically more attractive than consuming more grid power due to their lower costs (cf. Supporting Information). For the 2050 scenario, the further decrease in both production costs and carbon footprint compared to both prior scenarios can be explained by the power grid’s lowered carbon footprint in combination with lower investment costs for renewables and electrolysis. Towards minimal carbon footprints, we observe a much steeper increase in production costs in 2050 than in the other scenarios. This is because the plant must draw its entire power demand from its own renewable power plants to meet the carbon footprint constraint and does not

use electricity from the grid at all. Low carbon emissions associated with grid power result in much lower costs for very little additional emissions.

DSM-EL strictly dominates BC-EL in every considered scenario. For 2020 the BC-EL is almost identical to the corresponding point on the DSM-EL curve. In 2030 and 2050, the difference in both carbon emission mitigation and production cost is increasing. This shows that DSM can improve performance, especially in later scenarios, where grid power has higher fluctuations.

In summary, DSM and the investment in a system owned renewable energy power plants increase the economic viability of electrolytic hydrogen compared to steady-state operation. In relation to steady-state operation, the economic advantages of DSM-EL enhance for future scenarios. The pareto-optimal systems provide the optimal balance between electricity, electrolysis and hydrogen storage costs.

A limitation of this case study is that no comparison to alternate designs is made. A second case study is dedicated to thoroughly evaluate the proposed transition to green electrolytic hydrogen.

The cost for CO₂ mitigation increases alongside all scenarios, from 373 €/per tonne CO₂ avoided in scenario 2020 to 500 €/per tonne CO₂ avoided in 2030 and 650 € in 2050.

DSM-EL vs DSM-OS

In this section we analyse the economic and environmental viability of the proposed transition towards electrolytic hydrogen. For this purpose, we compare DSM-EL with DSM-OS. DSM-OS can choose to reduce iron ore by either synthesis gas or hydrogen. Synthesis gas can be produced with both natural gas and subsequent CCS or biogas reforming which is inherently carbon neutral. Pure hydrogen can only be produced via electrolysis. The optimisation results for DSM-OS are denoted by a dashed blue line in Figure 5. To get additional insight into the configuration of the optimal system plots displaying the energy input for the steel plant is given below in Figure 5.

Similarly to DSM-EL, the curves for DSM-OS show an increase in costs associated with CO₂ mitigation for all scenarios.

Comparing the results for DSM-EL and DSM-OS, all pareto-curves for the optimal system dominate the pareto-curves for green electrolytic hydrogen. For minimal production costs carbon emissions of DSM-OS are lower for both the 2020 as well as the 2030 scenario. This is not the case for 2050, where for minimal production costs DSM-OS has a slightly higher carbon footprint. The 2020 and 2030 results highlight the importance of low carbon emissions in the energy sector, as utilising grid-based power results in higher carbon footprints than utilising gas reforming. Renewable energy is widely used in 2050 [32] resulting in lower carbon emissions for electrolysis than for natural gas-based

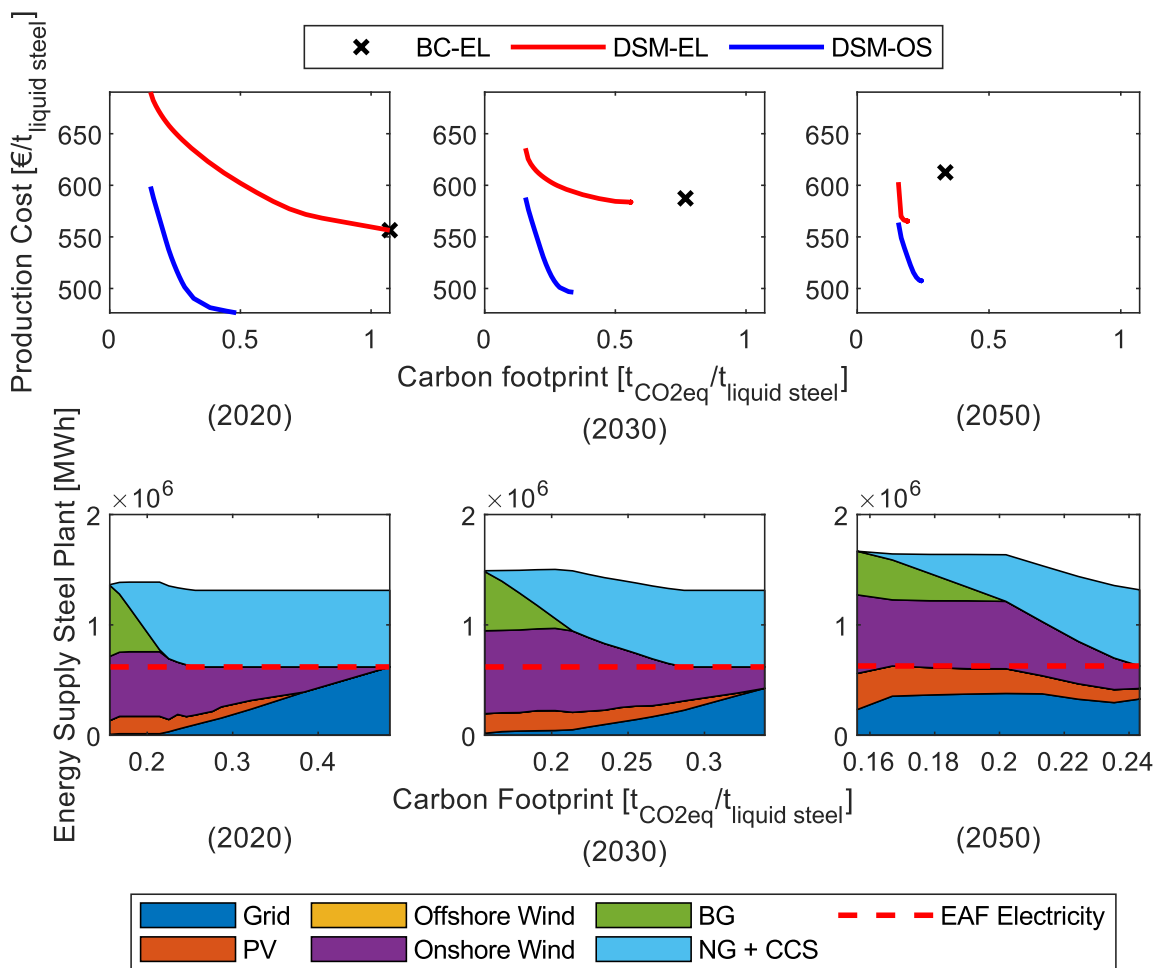


Figure 5: Results of the steelmaking optimisations. The first row presents the pareto fronts of the different systems in the years 2020, 2030 and 2050, respectively. The second row shows the corresponding energy input for the DSM-OS system.

iron reduction.

The subplots in the lower half of Figure 5 show that the DSM-OS changes the overall energy composition in the different scenarios. For all scenarios a fixed amount of electricity is needed to run the EAF, represented by a dashed red line. For the lowest possible production costs only natural gas-based synthesis gas is used as a reducing agent. For scenario 2020, moving up the DSM-OS pareto front is achieved by replacing grid power with renewable energy while still using only natural gas as synthesis gas feed. Lowering possible carbon emissions even further, an electrolysis unit is built first while almost simultaneously switching from natural gas to bio gas. The lowest possible carbon emission is achieved by powering the EAF purely with renewable energy and a mixture of biogas based synthesis gas and a small fraction of electrolytic hydrogen. The energy feed composition for scenario 2030 has a similar trajectory, though renewable energies are competing with grid power even for unlimited carbon emissions. Electrolysis are built

at slightly higher carbon emissions and subsequently, the highest carbon mitigation also contains a higher share of electrolytic hydrogen. Scenario 2050 continues this trend of earlier installation of electrolysis and higher competitiveness of renewable energies.

Another observation is a decreasing total energy demand of the system for increasing carbon footprints. This is caused by the replacement of electrolytic hydrogen with natural gas-based synthesis. Electrolysis efficiencies are lower than the those of synthesis gas production at 60% compared to 73% for natural gas-based and 68% for biogas based synthesis gas production.

Summary

In the first case study, we have shown the benefit of using DSM as a tool for both cost optimisation and carbon emission mitigation in the steelmaking process. Look-

ing at future scenarios, these benefits are further amplified. Comparison between DSM-EL and DSM-OS gives a clear overview of the technical challenges associated with the transition to green electrolytic hydrogen-based steelmaking. Lowering the carbon emission of grid power and electricity cost is one of the main challenges as these are the largest contributing cost factors (cf. Supporting Information). Given the prognosis that the mean electricity prices are expected to rise in the future but stronger fluctuations occur [32], a flexible process is necessary to minimise the main cost driver in the form of needed electricity.

Assessing the economic and environmental feasibility of the electrolytic system configuration, a comparison with fossil resource-based state of the art processes is reasonable. Germeshuizen et al. report cost and CO₂ emission data for the blast furnace and MIDREX process. Cost data is provided in cash production cost (CPC), thus excluding depreciation and fixed plant overhead and operating expenses [66]. We calculate the cash production costs by excluding depreciation related to the DRP and EAF, but including all other costs (for a detailed overview of the costs, cf. Supporting Information). Table 2 shows a comparison of literature data provided by Germeshuizen [66] and the results of this work.

	CPC ^a [$\frac{e}{t_{\text{liquid steel}}}$]	CF ^b [$\frac{kgCO_2}{t_{\text{liquid steel}}}$]
BF/BOF [66]	247	1848
MIDREX [66]	247	502
H ₂ based MIDREX [66]	282	184
DSM-EL min ^c	486	156
DSM-EL max ^c	364	1071
DSM-OS min ^c	382	156
DSM-OS max ^c	284	483

Table 2: Comparison of the optimisation results recalculated as cash production costs with literature data from Germeshuizen and Blom [66]. ^aCash production costs, ^bCarbon footprint, ^cCO₂ emissions scenario 2020.

It can be seen that DSM-EL can not be competitive against current processes in costs (364 vs. 282 USD/t liquid steel) for similar carbon emissions (156 vs 184). The optimal system performs worse than the hydrogen-based system proposed by Germeshuizen if the goal is to minimise carbon emissions. It should be noted that we currently include high investment costs for renewable energies and the biogas SMR and thus a difference of 140 € shows the promise of the presented DSM-OS system.

5.2. Ammonia

The ammonia section is structured as follows: In the first section the economic and environmental benefits for the ammonia system are assessed by comparing BC-EL to the demand side managed electrolysis (DSM-EL). The second section is dedicated to analysing how DSM-EL performs in comparison to the optimal ammonia system (DSM-OS).

DSM-EL vs BC-EL

Pareto fronts of the optimisation results are visualised in the first row of Figure 6 and show the production cost and the carbon footprint in the considered scenarios.

Similar to the steelmaking process the DSM-EL pareto fronts have increased production costs for lower carbon footprints. A trend towards lower production cost for future DSM-EL scenarios can be observed despite increasing power grid prices. The decreasing investment cost for electrolysis and for the considered renewable energy plants are the main cause for this trend and can be seen in the Supporting Information. The points with minimal production costs are decreasing in carbon footprint as well which can be explained by the lower carbon footprint of the power grid in future scenarios.

Comparing the cost-optimal point of the DSM-EL curve to the BC-EL point for each scenario the production cost decreases by 1.4%, 2.7% and 30.0% and the carbon footprint by 0.08%, 29.9% and 88.0%, respectively. This shows the benefits of DSM to be increasing in future scenarios.

DSM-EL vs DSM-OS

In order to assess the potential of green electrolytic hydrogen DSM-EL is compared to DSM-OS in Figure 6. To give insights into the used technologies information about the origin of hydrogen in the OS is provided in the respective subplots of Figure 6, below.

Figure 6 shows that in the 2020 scenario, the DSM-OS strictly dominates the DSM-EL as it has a lower production cost for all carbon footprints. For a lower carbon footprint the gap between the two cost curves decreases. DSM-OS behaves linearly before transitioning into a steeper curve. The linear part is a result of the replacement of natural gas by biomethane which can be seen below. When all natural-gas is replaced by biomethane, electrolysis is used to further decrease the emissions until CCS instead of electrolysis becomes the more economical option.

In scenario 2030 DSM-OS has lower production costs than DSM-EL for most carbon footprints, but approaching minimal carbon emissions both converge. In this context DSM-OS finds the economic optimum by installing electrolysis instead of CCS for the low carbon footprint. The electricity for this is mainly supplied from built renewable energy

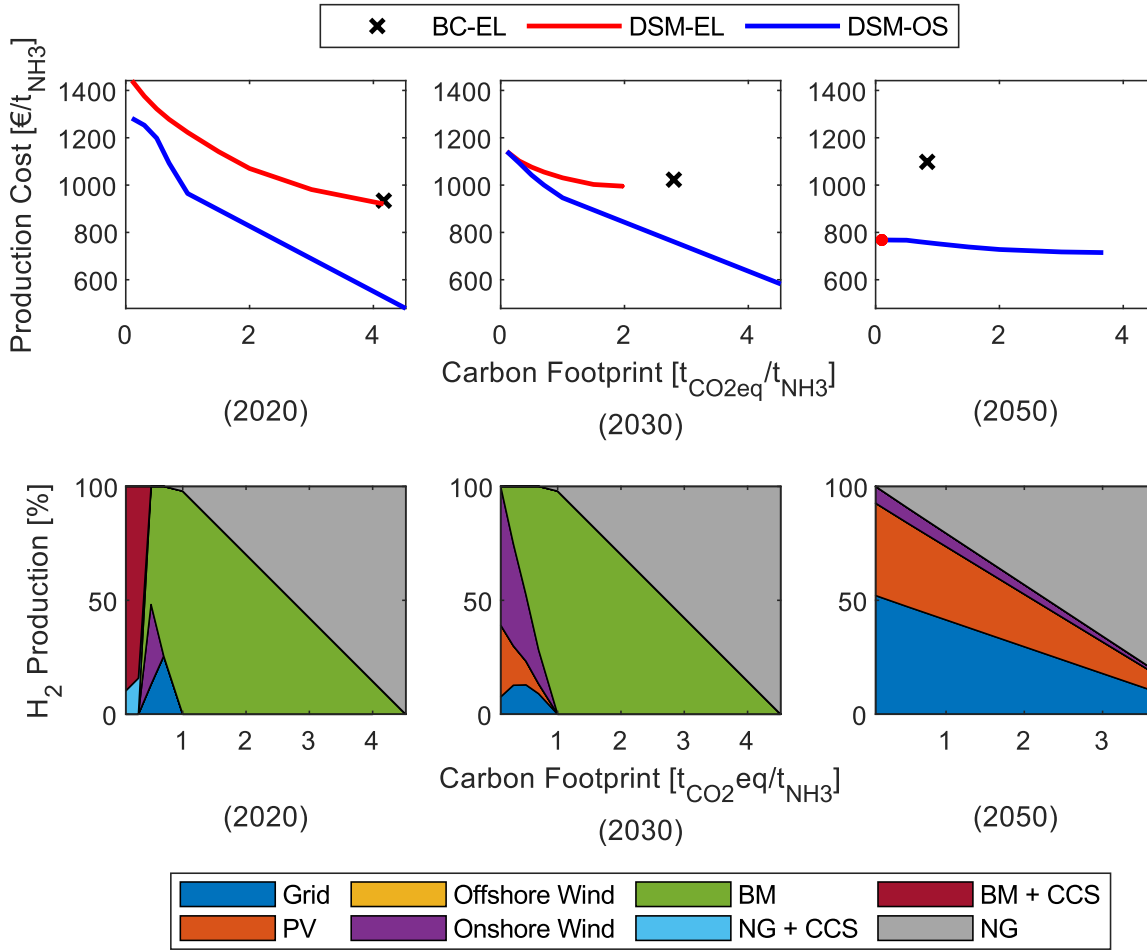


Figure 6: Results of the ammonia optimisations. The first row presents the pareto fronts of the different systems in the years 2020, 2030 and 2050, respectively. The second row shows the corresponding hydrogen origin for the DSM-OS system.

plants, because the carbon footprint of the power grid is too high. The linear characteristic at high carbon footprint has the same reason as in 2020.

For the 2050 scenario curves are flattened out indicating that decreasing the carbon footprint does not come along with a large increase in production costs. Investigating the hydrogen origin reveals that electrolysis is always built in every optimal system. Also, the DSM-EL curve is part of the DSM-OS curve showing that electrolysis only is the cost-optimal system for minimal carbon emissions. Both observations can be traced back to the cost reduction for both electrolysis and renewable energy plants in 2050 (cf. Supporting Information).

Across the scenarios both curves become flatter and approach each other concluding that the gap between electrolysis and optimal system configuration becomes smaller. The choice of economical optimal hydrogen sources shifts from natural gas to renewable energy and electricity. While

biomethane is the optimal choice for reducing the carbon footprint in 2020 and 2030 it is superseded by electrolysis in 2050. This is mainly based on the cost reduction of electrolysis and PV plants in addition to a low-carbon power grid and increasing CO₂ taxes. A minor factor is the increasing natural gas price.

Dynamic operation of the ammonia production

As described in the modelling section, DSM optimises the operational schedules in terms of the production rates of the different plants. In chapter 5.2 the cost and economical advantages for DSM have already been elaborated. An example of a resulting load profile is presented in the following.

Fig 7 shows the plant loads for an exemplary interval. The electrolysis operates dynamically and has a cyclic load

profile with cycles of 24 hours. To benefit from the low grid power prices the load is maximised during the day and turning to minimum at night. Contrary to this, the ammonia plant does not have the corresponding flexibility due to longer settling times for production rate changes [59]. For this reason a hydrogen tank is needed for a more flexible operation of the electrolysis.

If the ammonia plant was able to operate more dynamically and could change from minimum to maximum load in a day cycle a much smaller hydrogen tank would be needed and a much cheaper ammonia tank could be used as a buffer for the dynamic load.

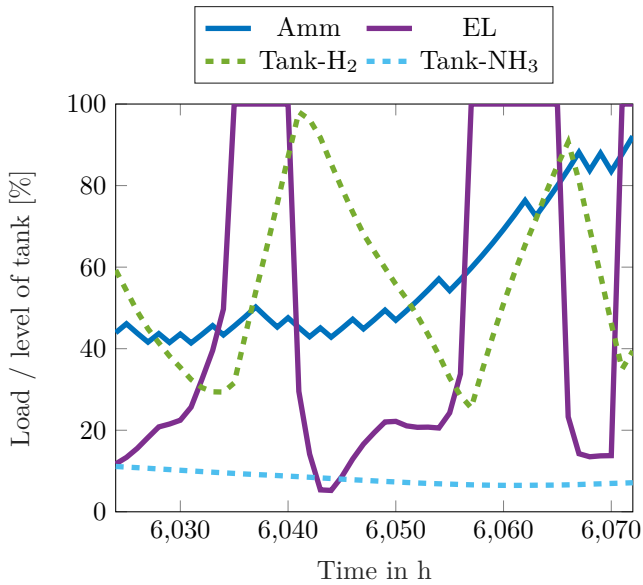


Figure 7: Load of the electrolysis, the ammonia plant and the level of the hydrogen and ammonia tank for BC-EL in 2030

Summary: results for the ammonia system

For the transition towards green hydrogen in the ammonia system the results show that under current conditions it is not economically viable to change towards electrolytic hydrogen production. CCS can be used to reduce the carbon footprint, but it is only optimal if the production is completely shifted to biomethane and a really small footprint is desired. Moreover, using biomethane to reduce the carbon footprint to an intermediate level seems to present a more acceptable short term option.

The optimisation suggests that with the prognosticated cost and market data, electrolysis will already be part of the optimal ammonia production system by 2050, even if the cost is taken as the only decision criteria. It was also shown that the cost of reducing carbon emissions for the lowest cost system (DSM-OS) is going down heavily, with a value of around 138 €/t_{CO₂ avoided} in 2020, 103 €/t_{CO₂ avoided} in 2030 to a value of around 15€/t_{CO₂ avoided} in 2050. The val-

ues of 2020 and 2030 can be achieved by using biomethane, the value of 2050 by using electrolysis.

An almost carbon-free ammonia production with a carbon footprint of under 0.1 t_{CO₂}/t_{NH₃} could be achieved by 2050 if electrolysis is used.

The current ammonia footprint in Europe is estimated to be 3.7 t_{CO₂}/t_{NH₃} [67] which is close to the found value of 4.52 t_{CO₂}/t_{NH₃} for a state of the art process only using natural gas in 2020. The European goal is to decrease the industry sectors carbon emissions by around 85% from 2020 to 2050 [68]. In the context of ammonia production and the results of this work this would imply reducing the carbon footprint from 4.52 to 0.68 t_{CO₂}/t_{NH₃}. For this carbon footprint the optimal system in 2050 uses electrolysis for around 85% of the hydrogen production. This result shows the necessity of introducing green electrolytic hydrogen into ammonia production.

5.3. Comparison of steel and ammonia

At the current time, the transition to electrolytic hydrogen is economically not desirable for both steelmaking and ammonia production.

Biomass-based hydrogen is an economical and ecological option to reduce the carbon footprint of both processes as long as the decarbonisation of the energy sector is not completed.

Comparison of DSM-EL and DSM-OS systems allows quantification of possible economical and environmental improvements. The DSM-EL curves are closer to the DSM-OS ones for the ammonia process than for the steelmaking process. Using a considerable amount of electrolytic hydrogen leads to the lowest production costs for all investigated carbon footprints of ammonia in the 2050 scenario. Whereas, in steelmaking this only holds for lower carbon footprints. Additionally, the ammonia process accounts for a much larger fraction of the European industrial sector's GHG emissions. Therefore, ammonia is the more promising process to reduce carbon emission while keeping the additional production cost low.

5.4. Limitations of hydrogen production

All sources for low carbon hydrogen face drawbacks and trade-offs are unavoidable. In the case of CCS, we emphasise the technologies prematurity as it has never been carried out on a large scale [65]. Further, concerns among the population over onshore underground storage of CO₂ may hinder its implementation [69]. Green hydrogen also faces limitations. The production of biomass is limited by agriculture and forestry. The current hydrogen duty of the European steelmaking and ammonia industry would consume around 4% of the entire biomass potential of the EU 26 [9] but 49% of the total European biomass production in 2015 [70]. Not only biomass but renewable energy in gen-

eral is limited. A maximum potential energy generation of 1700 TWh/a from renewable energies (including biomass) is estimated for Germany [71]. This amount could only cover 45% of the German primary energy consumption in 2016 [72]. Hence, the energy consumption must decrease significantly which competes with electrolytic hydrogen generation, especially as PEM electrolyzers have an energy efficiency of approximately 60%. The latter problem may be alleviated by solid oxide electrolyzers which can achieve an efficiency of almost 100% [7, 73]. However, this technology is still in the pilot stage and not yet available.

6. Conclusion & Outlook

We investigated the economic and environmental feasibility of transitioning industrial steel and ammonia production from fossil resources to green electrolytic hydrogen. To this end, we modelled a steel plant, an ammonia plant and a biogas reformer. A detailed shaft furnace model was implemented in MATLAB and connected to the DRP via the ASPEN PLUS/MATLAB interface. We compared the production cost of steel and ammonia production utilising green electrolytic hydrogen only with the production costs of respective processes utilising all available low carbon hydrogen sources. Bi-objective optimisation of production costs and carbon emissions was utilised for determining optimal plant scheduling and sizing. The optimisation problem was modelled and solved in GAMS. We evaluated future trends by putting scenarios for 2020, 2030 and 2050 in contrast. For a grass-roots design of a steel or ammonia plant in an energy system similar to Germany, we found that:

- The power price and the carbon footprint of grid power are economical and environmental barriers for electrolytic hydrogen production. Electrolytic hydrogen is not suitable for decarbonising the industry in the considered case studies before 2050. This is due to the hydrogen's carbon footprint being highly dependent on the carbon footprint of electricity. Thus, the decarbonisation of the energy sector should receive priority.
- Green hydrogen from biomass is a more attractive alternative for short term reduction of the carbon footprint than electrolysis. Additionally, blue hydrogen from natural gas with subsequent CCS qualifies as an economical alternative for steelmaking. However, the environmental impact of CCS requires further investigation.
- Pure hydrogen-based iron reduction is neither competitive in costs nor carbon footprint with synthesis gas based iron reduction in all considered scenarios.
- DSM enhances the economic viability of electrolysis.

In the 2050 scenario, electrolysis can compete with other hydrogen sources and is part of the optimal ammonia production system. This can only be achieved by DSM while steady state electrolysis is not attractive.

While the evaluated optimal systems for transitioning steel and ammonia production to low carbon emission feeds featured hydrogen or synthesis gas from all allowed sources, we observed a trend towards electrolytic hydrogen for 2050. However, we investigated future power prices by its marginal costs. Power taxes are likely to be an economic obstacle for electrolytic hydrogen.

Short-term research should focus on determining the optimal plant setup while considering the change of the market situation over the plant lifetime utilising the developed optimisation model. Additionally, the balancing market for power could be introduced to the model since balancing power offers another potential to increase the economic viability of electrolysis by DSM.

Supporting Information is attached

References

- [1] European Commission, What is the European Green Deal?, 2019. URL: https://ec.europa.eu/commission/presscorner/detail/en/fs_19_6714.
- [2] European Commission, Causes of climate change, 2020. URL: https://ec.europa.eu/clima/change/causes_en.
- [3] European Environment Agency, EEA report No 16/2019: Annual European Union approximated greenhouse gas inventory for the year 2018, 2018.
- [4] Francesco Dolci, Green hydrogen opportunities in selected industrial processes (2018).
- [5] International Renewable Energy Agency, Hydrogen from renewable power: Technology outlook for the energy transition, 2018.
- [6] M. Kopp, D. Coleman, C. Stiller, K. Scheffer, J. Aichinger, B. Schepat, Energiepark Mainz: Technical and economic analysis of the worldwide largest power-to-gas plant with PEM electrolysis, *International Journal of Hydrogen Energy* 42 (2017) 13311–13320.
- [7] A. Buttler, H. Spliethoff, Current status of water electrolysis for energy storage, grid balancing and sector coupling via power-to-gas and power-to-liquids: A review, *Renewable and Sustainable Energy Reviews* 82 (2018) 2440–2454.
- [8] Tom Smolinka, Nikolai Wiebe, Philip Sterchele, Studie IndWEde Industrialisierung der Wasser-Elektrolyse in Deutschland: Chancen und Herausforderungen für nachhaltigen Wasserstoff für Verkehr, Strom und Wärme, 2018.
- [9] A. Tilche, M. Galatola, The potential of bio-methane as bio-fuel/bio-energy for reducing greenhouse gas emissions: a qualitative assessment for Europe in a life cycle perspective, *Water Science and Technology: a journal of the International Association on Water Pollution Research* 57 (2008) 1683–1692.
- [10] N. Abatzoglou, S. Boivin, A review of biogas purification processes, *Biofuels, Bioproducts and Biorefining* 3 (2009) 42–71.
- [11] O. W. Awe, Y. Zhao, A. Nzihou, D. P. Minh, N. Lyczko, A review of biogas utilisation, purification and upgrading technologies, *Waste and Biomass Valorization* 8 (2017) 267–283.
- [12] J. DUFOUR, D. SERRANO, J. GALVEZ, J. MORENO, C. GARCIA, Life cycle assessment of processes for hydrogen production. environmental feasibility and reduction of greenhouse gases emissions, *International Journal of Hydrogen Energy* 34 (2009) 1370–1376.
- [13] GasTerra, Hydrogen and CCS: a smart combination, 11.02.2020. URL: <https://www.gasterra.nl/en/news/hydrogen-and-ccs-a-smart-combination>.
- [14] C. Yilmaz, et al., Modeling and simulation of hydrogen injection into a blast furnace to reduce carbon dioxide emissions, *Journal of Cleaner Production* 154 (2017) 488–501.
- [15] H. Nogami, Y. Kashiwaya, D. Yamada, Simulation of blast furnace operation with intensive hydrogen injection, *ISIJ International* 52

- (2012) 1523–1527.
- [16] K. Meijer, M. Denys, J. Lasar, J.-P. Birat, G. Still, B. Overmaat, Ulcos: ultra-low co 2 steelmaking, *Ironmaking & Steelmaking* 36 (2009) 249–251.
- [17] J.-P. Birat, Update on the ulcos program, ArcelorMittal ESTEP Report (2011).
- [18] P. R. Behera, Hydrogen plasma smelting reduction of fe₂o₃, *Metalurgical and Materials Transactions B* 50 (2019) 262–270.
- [19] H. Hamadeh, Modélisation mathématique détaillée du procédé de réduction directe du minerai de fer, Français, 2017.
- [20] D. Wagner, Etude expérimentale et modélisation de la réduction du minerai de fer par l'hydrogène (2008).
- [21] V. Vogl, M. Åhman, L. J. Nilsson, Assessment of hydrogen direct reduction for fossil-free steelmaking, *Journal of Cleaner Production* 203 (2018) 736–745.
- [22] thyssenkrupp Steel Europe, Hydrogen instead of coal. thyssenkrupp Steel launches pioneering project for climate-friendly steel production at its Duisburg site, 2019.
- [23] L. Wang, M. Xia, H. Wang, K. Huang, C. Qian, C. T. Maravelias, G. A. Ozin, Greening ammonia toward the solar ammonia refinery, *Joule* 2 (2018) 1055–1074.
- [24] A. Nielsen (Ed.), *Ammonia: Catalysis and Manufacture*, Springer Berlin Heidelberg, Berlin, Heidelberg, 1995. doi:10.1007/978-3-642-79197-0.
- [25] P. Tunå, C. Hultheberg, S. Ahlgren, Techno-economic assessment of nonfossil ammonia production, *Environmental Progress & Sustainable Energy* 33 (2014) 1290–1297.
- [26] Agora Energiewende, 22.01.2020. URL: <https://www.agora-energiewende.de/service/agorameter>.
- [27] Fraunhofer Institute For Solar Energy Systems ISE, Levelized Cost of Electricity- Renewable Energy Technologies, 2018.
- [28] J. Burre, et al., Power-to-x: Between electricity storage, e-production, and demand side management, *Chemie Ingenieur Technik* 92 (2020) 74–84.
- [29] L. C. Brée, K. Perrey, A. Bulan, A. Mitsos, Demand side management and operational mode switching in chlorine production, *AIChE Journal* 65 (2019) e16352.
- [30] N. Baumgärtner, et al., Design of low-carbon utility systems: Exploiting time-dependent grid emissions for climate-friendly demand-side management, *Applied Energy* 247 (2019) 755–765.
- [31] F. Klauke, T. Karsten, F. Holtrup, E. Esche, T. Morosuk, G. Tsatsaronis, J.-U. Repke, Demand response potenziale in der chemischen industrie, *Chemie Ingenieur Technik* 89 (2017) 1133–1141.
- [32] F. Böing, A. Regett, Hourly co₂ emission factors and marginal costs of energy carriers in future multi-energy systems, *Energies* 12 (2019) 2260.
- [33] Béchara, et al., Optimization of the iron ore direct reduction process through multiscale process modeling, *Materials (Basel, Switzerland)* 11 (2018).
- [34] I. Aspen Technology, Aspen plus v.10 (2020).
- [35] D. R. Parisi, M. A. Laborde, Modeling of counter current moving bed gas-solid reactor used in direct reduction of iron ore, *Chemical Engineering Journal* 104 (2004) 35–43.
- [36] Adris, A. M., Pruden, B. B., Lim, C. J., Grace, J. R., On the reported attempts to radically improve the performance of the steam methane reforming reactor, 1996.
- [37] K. Roh, J. H. Lee, R. Gani, A methodological framework for the development of feasible co₂ conversion processes, *International Journal of Greenhouse Gas Control* 47 (2016) 250–265.
- [38] P. Adler, E. Billig, A. Brosowski, J. Daniel-Gromke, I. Falke, E. Fischer, Leitfaden Biogasaufbereitung und -einspeisung, 5., vollständig überarbeitete auflage ed., Fachagentur für Nachwuchsende Rohstoffe e. V. (FNR), Gülzow-Prüzen, 2014. URL: <https://edocs.tib.eu/files/e01fb16/868893196.pdf>. doi:10.2314/GBV:868893196.
- [39] Benschop, Alex, Jannssen, Koksberg, Deriwala, Munaf, Abry, Ray, Ngai, Charles, New commercial process for h₂s removal from high pressure natural gas: The shell-thiopaq gas desulfurisation process (2020).
- [40] M. R. Abu-Zahra, et al., Co₂ capture from power plants, *International Journal of Greenhouse Gas Control* 1 (2007) 135–142.
- [41] A. Bahadori, H. B. Vuthaluru, Simple methodology for sizing of absorbers for teg (triethylene glycol) gas dehydration systems, *Energy* 34 (2009) 1910–1916.
- [42] A. Shams, et al., Modeling and simulation of the midrex shaft furnace: Reduction, transition and cooling zones, *JOM* 67 (2015) 2681–2689.
- [43] P. Palacios, et al., Iron ore reduction by methane partial oxidation in a porous media, *International Journal of Hydrogen Energy* 40 (2015) 9621–9633.
- [44] Alamsari, et al., Study of the effect of reduced iron temperature rising on total carbon formation in iron reactor isobaric and cooling zone, *Advances in Mechanical Engineering* 2 (2010) 192430.
- [45] B. Alamsari, et al., Heat and mass transfer in reduction zone of sponge iron reactor, *ISRN Mechanical Engineering* 2011 (2011) 1–12.
- [46] H. Hamadeh, et al., Detailed modeling of the direct reduction of iron ore in a shaft furnace, *Materials (Basel, Switzerland)* 11 (2018).
- [47] MATLAB, version 9.7 (R2019b), The MathWorks Inc., 2019.
- [48] Linde, Ammonia, 2020. URL: https://www.linde-engineering.com/en/process-plants/hydrogen_and_synthesis_gas_plants/gas_products/ammonia/index.html.
- [49] James M. Douglas, *Conceptual design of chemical process*, McGraw Hill, 1988.
- [50] R. Turton, R. Bailie, W. Whiting, J. Shaeiwitz, D. Bhattacharyya, *Analysis, Synthesis, and Design of Chemical Processes*, Fourth Edition, 4th edition ed., Prentice Hall, 2012.
- [51] R. R. T. Melin, *Membranverfahren*, Springer Berlin Heidelberg, Berlin, Heidelberg, 2007. doi:10.1007/978-3-540-34328-8.
- [52] P. Bartels, A feasibility study of implementing an ammonia economy (2008).
- [53] E. R. Morgan, J. F. Manwell, J. G. McGowan, Sustainable ammonia production from u.s. offshore wind farms: A techno-economic review, *ACS Sustainable Chemistry & Engineering* 5 (2017) 9554–9567.
- [54] M. M. F. Hasan, et al., Nationwide, regional, and statewide co₂ capture, utilization, and sequestration supply chain network optimization, *Industrial & Engineering Chemistry Research* 53 (2014) 7489–7506.
- [55] Murthy Konda, et al., Optimal transition towards a large-scale hydrogen infrastructure for the transport sector: The case for the netherlands, *International Journal of Hydrogen Energy* 36 (2011) 4619–4635.
- [56] R. Millner, et al., Further opportunities of competitiveness improvements for direct reduction plants, *BHM Berg- und Hüttenmännische Monatshefte* 164 (2019) 274–280.
- [57] V. S. D. Stolten (Ed.), *Transition to Renewable Energy Systems*, Wiley-VCH, Weinheim, 2013.
- [58] S. Schulte Beerbühl, M. Fröhling, F. Schultmann, Combined scheduling and capacity planning of electricity-based ammonia production to integrate renewable energies, *European Journal of Operational Research* 241 (2015) 851–862.
- [59] W. L. Luyben, Plantwide control of a coupled reformer/ammonia process, *Chemical Engineering Research and Design* 134 (2018) 518–527.
- [60] GAMS Software GmbH, Cplex 12, 07.12.2019. URL: https://www.gams.com/latest/docs/S_CPLEX.html.
- [61] Mitra, et al., Optimal production planning under time-sensitive electricity prices for continuous power-intensive processes, *Computers & Chemical Engineering* 38 (2012) 171–184.
- [62] I. Tsiropoulos, et al., Cost development of low carbon energy technologies, 2017.
- [63] M. Schlesinger, *Entwicklung der energiemärkte - energiereferenzprognose*, 2014.
- [64] Agency for Renewable Resources, *Bioenergy in germany facts and figures* 2019 (2019).
- [65] M. Bui, et al., Carbon capture and storage (ccs): the way forward, *Energy & Environmental Science* 11 (2018) 1062–1176.
- [66] L. M. Germeshuizen, P. Blom, A techno-economic evaluation of the use of hydrogen in a steel production process, utilizing nuclear process heat, *International Journal of Hydrogen Energy* 38 (2013) 10671–10682.
- [67] F. Paulot, et al., Ammonia emissions in the united states, european union, and china derived by high-resolution inversion of ammonium wet deposition data: Interpretation with a new agricultural emissions inventory (masage_nh3), *Journal of Geophysical Research: Atmospheres* 119 (2014) 4343–4364.
- [68] *Going climate-neutral by 2050: A strategic long-term vision for a prosperous, modern, competitive and climate-neutral EU economy*, Publications Office of the European Union, Luxembourg, 2019.
- [69] R. Krupp, *Geologische kurzstudie zu den bedingungen und moeglichen auswirkungen der dauerhaften lagerung von co2 im untergrund*. (2010).
- [70] N. Scarlat, J.-F. Dallemand, F. Fahl, *Biogas: Developments and perspectives in europe*, *Renewable Energy* 129 (2018) 457–472.
- [71] Estermann, et al., *Kurzstudie power-to-x* (2017).
- [72] Statistisches Bundesamt, *Statistisches Jahrbuch* 2019, Wiesbaden, 2019.
- [73] D. Stolten (Ed.), *Hydrogen and fuel cells: Fundamentals, technologies and applications ; contributions to the 18th World Hydrogen Energy Conference* 2010, Essen, 2. reprint ed., Wiley-VCH, Weinheim, 2011.